Chiang Mai J. Sci. 2021; 48(2) : 405-419
http://epg.science.cmu.ac.th/ejournal/
Contributed Paper

Antioxidant and Cytotoxicity Activities of Butylated Hydroxytoluene Ligands Capped Gold Nanoparticles

Mohd Hafiz Ahmad [a], Wageeh A. Yehye [a], Noorsaadah Abd. Rahman [b], Lina A. Al-Ani [a], Mohd Rafie Johan [a], Jun Lu [c] and Najihah M. Hashim*[d,e]

[a] Nanotechnology & Catalysis Research Centre (NANOCAT), Universiti Malaya, Block 3A, Inst. of Graduate Studies Building, 50603 Kuala Lumpur, Malaysia.

[b] Department of Chemistry, Faculty of Science, Universiti Malaya, 50603 Kuala Lumpur, Malaysia.

[c] School of Science and School of Interprofessional Studies, Faculty of Health and Environmental Sciences, Auckland University of Technology, Auckland 1142, New Zealand.

[d] Department of Pharmaceutical Chemistry, Faculty of Pharmacy, Universiti Malaya, 50603 Kuala Lumpur, Malaysia.

[e] Centre for Natural Products Research and Drug Discovery (CENAR), Universiti Malaya, 50603 Kuala Lumpur, Malaysia.

*Author for correspondence; e-mail: najihahmh@um.edu.my

Received: 16 September 2020
Revised: 17 November 2020
Accepted: 20 November 2020

ABSTRACT

The new potent nano-antioxidant of sulfur-containing butylated hydroxytoluene ligands (S-BHTLs)-conjugated with gold nanoparticles, Au-S-BHTLs, was synthesized by a conjugation of sulfur-containing ligands derived from BHT on the surface of gold nanoparticles (AuNPs). The in-house developing eight sulfur-containing BHT-ligands (S-BHTLs) were used for further study on functionalization with AuNPs and their biological activities. The antioxidant and cytotoxic abilities of eight types of Au-S-BHTLs such as compound **Au-2a**, **Au-2b**, **Au-3a**, **Au-3b**, **Au-4a**, **Au-4b**, **Au-5a** and **Au-5b** were tested by DPPH$^{\bullet}$ (2,2-diphenyl-1-picrylhydrazyl) radical scavenging and MTT assays against HT29 (human colorectal adenocarcinoma) and MCF7 (human breast adenocarcinoma). Based on the results, it was revealed that nanocomposites **Au-5a** and **Au-3a** attained over 50% lower IC_{50} values against free radical than the un-functionalized AuNPs. Meanwhile, nanocomposite **Au-2b** showed the highest cytotoxicity effect against both cancer cell lines. Selectivity and safety towards non-tumorgenic cell lines were also evaluated and proved superior selectivity index (SI) of all nanocomposites (SI > 2.00) against both cancer cells except **Au-5b** (SI = 1.87) against MCF7. Hence, the functionalization of S-BHTLs with gold nanoparticles has increased the selectivity of nanocomposites and enhanced the antioxidant potentials to become useful and promising anticancer agents.

Keywords: gold nanoparticles, Au-S-BHTLs, DPPH, HT29, MCF7

1. INTRODUCTION

The increased attention paid to drug development and modern therapeutic modalities is explained by the need to implement advanced drug technologies in confronting the higher incidence and mortality rates of various diseases [1]. Oxidative stress state which reflects the

increased reactive oxygen species (ROS) levels and/or hindered anti-oxidants levels has been implicated in diverse pathologies, including cancer disease [2]. As a consequence, the current trend of drug development is keen on identifying effective antioxidants formulations with hope to achieve enhanced activity and reduced possible toxicities.

Among the most common used synthetic antioxidants is butylated hydroxytoluene (BHT), with many reports confirming the potent antioxidant activity in various industrial applications such as food, oil, and cosmetics industries [3]. In addition, this phenolic synthetic antioxidant has been also applied in therapeutic fields, however, certain features of volatility and high-temperature instability, as well as toxicities and safety concerns have greatly limited the effective therapeutic application [4]. To this end, current research is focusing on designing and synthesizing new BHT-derivatives to enhance anti-oxidant and therapeutic activities, as well as reducing toxic side effects [5]. Nanotechnology has recently presented a superb option in this path, with many nanomaterials and different hybridization and functionalization methods [6]. Therefore, the foreseeable future of pharmaceutical and biotechnology industries landscape has been expected to change through the nanotechnology application on drug delivery [7]. Past research reported that nanoparticles improved the activity of known molecules by decreasing the toxicity, increasing the efficiency and allowing a better control of the drug plasma levels [8].

Gold nanoparticles (AuNPs) are among the most magnificent of metal-based nanomaterials, due to their unique physical, chemical, electronic and optical properties [9]. The AuNPs possess efficient and excellent therapeutic effects against several diseases and have shown excellent potential as drug delivery scaffolds due to their non-immunogenic and non-toxic properties, [10]. The functionalization of organic molecules onto the surface of AuNPs provides highly potential and functional therapeutic agent to treat several diseases [11, 12] as well as to increase their stability and biocompatibility [13]. Moreover, AuNPs are also reported to enhance the reactivity and improve the antioxidant activity of conjugated ligands [14]. As reported by Selim and her colleagues [15], AuNPs show therapeutic potential through cytotoxic effect against human breast cancer cells (MCF7). AuNPs were also used to improve the anticancer efficacy of 5-fluorouracil against colorectal cancer cells through conjugation on NPs surface incorporating two thiol containing ligands, glutathione (GSH) and thioglycolic acid (TGA) [16].

In the present study, we aim to exploit the potent antioxidant activity of BHT, while surpassing its disadvantageous toxicity and limitations. We report an integration strategy combining sulfur-containing BHT-ligands with AuNPs (Au-S-BHTLs) by incorporating our previous work's thiol ligands derived from BHT [17] onto the surface of AuNPs. Herein, AuNPs as the platform can provide an eminent route in improving the safety profile of the whole system. Additionally, AuNPs presence is proposed to increase the antioxidant and cytotoxicity activities. The 2,2-diphenyl-1-picrylhydrazyl radical ($DPPH^{\bullet}$) assay was used to verify the antioxidant activity of Au-S-BHTLs and their cytotoxicity effect was evaluated on human colon adenocarcinoma (HT29) and human breast adenocarcinoma (MCF7) cancer cell lines. Hence, the combination of BHT moiety with AuNPs may produce an excellent compound for enhanced antioxidant properties as well as in anti-cancer therapy.

2. MATERIALS AND METHODS

Materials and solvents were purchased from Sigma-Aldrich. Hexane, chloroform, diethyl ether and methanol used were in analytical grade. Gold hydrochlorate and trisodium citrate were used as a precursor and reducing agent for synthesis of gold nanoparticles, respectively. Sulfur-containing BHT ligands were used as surfactant conjugated on gold nanoparticles surface. The HT29 (colon adenocarcinoma), MCF7 (breast adenocarcinoma),

CCD 841 (colon cell and MCF10A (breast cell) cells were obtained from American Type Culture Collection (ATCC, Manassas, USA).

2.1 Synthesis of Gold Nanoparticles via The Turkevich Method

AuNPs were synthesized according to Li and his co-workers by a reduction of gold hydrochlorate using trisodium citrate [18]. The 300 ml of 1 mM $HAuCl_4$ was brought to boil while being stirred and refluxed, and then 30 ml of 38.8 mM trisodium citrate was quickly poured into the boiling $HAuCl_4$ solution. The solution was continuously stirred and heated until the color turned deep red. Then, the solution was cooled to room temperature; and 20 μm syringe filter was used to filter the solution and was stored in refrigerator at 4 °C.

2.2 Synthesis of Sulfur-Containing BHT-Ligands Functionalized Gold Nanoparticles

The thiol groups are strong enough to immobilize on the surface of metal nanoparticles because of the Au-sulfur interaction. The Au-S-BHTLs were prepared by published routes [19] with the modification approaches, 1 ml of AuNPs solution (about 3.2 nM) was mixed with S-BHTLs solution (5×10^{-4} M, 100 μl) and stirred for 30s. Then, the mixture solution was left to react for overnight at 4 °C.

2.3 TEM Characterization of Au-S-BHTLs

TEM observations spectra were performed on a (HR-TEM; JEOL JEM-2100F). The nanoparticles were deposited onto Lacey 300 Mesh copper grids from diluted chloroform suspension and then dried in the air.

2.4 SEM Characterization of Au-S-BHTLs

The field-emission scanning electron microscope (FESEM; FEI Quanta 200F, USA) operating at 10kV and 100 Pa, *i.e.*, low vacuum condition was used to identify the surface morphology of the gold nanoparticles and Au-S-BHTLs. The Au-S-BHTLs was deposited onto conductive carbon tape before the FESEM imaging.

2.5 Antioxidant Activity

The Au-S-BHTLs were evaluated in terms of radical scavenging or hydrogen donating ability using DPPH assay protocol reported by Gorinstein *et al.*, [20]. The colour changes of reaction mixture against the blank were measured at 517 nm. All samples with gradually increasing concentrations (10, 50, 100, 200, 400 and 600 μg/ml) was added with 0.1 mM of DPPH solution in methanol. Meanwhile, AuNPs were used as positive control for the Au-S-BHTLs antioxidant test. The decolourization percentage of sample against DPPH was calculated as per below equation:

$$\text{DPPH scavenging effect} = \frac{A_{control} - A_{sample}}{A_{control}} \times 100\%$$

$A_{control}$ is denoted as the absorbance of the control reaction and, A_{sample} is as the absorbance of the tested compounds measured at 517 nm. The tests were conducted in triplicate.

2.6 Cytotoxicity Assay

In the present study, the cytotoxicity effect of Au-S-BHTLs was evaluated using HT29 (colon adenocarcinoma) and MCF7 (breast adenocarcinoma). Cancer cell line's non-tumorigenic counterparts such as CCD 841 (colon cell) and MCF10A (breast cell) were also employed to explore the selectivity. Cells were cultured in RPMI-1640 medium (SigmaAldrich, USA), supplemented with 10% fetal bovine serum (Gibco,USA), and 1% Pen-Strep antibiotic (10,000 units penicillin-10 mg streptomycin/mL, SigmaAldrich) in a 37 °C humidified 5% CO_2 incubator (ThermoFischer Scientific, USA).

2.6.1 MTT assay

Based on previous protocols [21], the cells were plated into 96-well plates at the density of 5000 cells/well in the final volume of 100 μl culture medium per well. Then, AuNPs and Au-S-BHTLs

were used to treat the cells at gradually increasing concentrations (62.5, 125, 250, 500 and 1000 μg/ml) and maintained at 37°C with 5% CO_2 for 24 hours on the following day. Cells without treatment were used as negative control. Each well was added with 10 μl of MTT reagent (5 mg/ml) at the end of the incubation period and incubated at the same condition for 4 hours. The 100 μl of dimethylsulphoxide (DMSO) was added into each well after the supernatant was removed, and the absorbance of treated cells was determined using microplate reader (Infinite-M200Pro-TECAN) at 570 nm. The experiment was conducted in triplicate and the equation below was used to calculate the cellular viability accordingly:

$$\text{Cell viability (\%)} = \frac{\text{Sample absorbance}}{\text{Control absorbance}} \times 100$$

2.6.2 Selectivity index

Based on previous reports [22], the selectivity index (SI) was calculated using the equation as described below:

$$SI = \frac{IC_{50} \text{ of tested compound on normal cell line}}{IC_{50} \text{ of tested compound on cancer cell}} \times 100$$

3. RESULTS AND DISCUSSION

3.1 Synthesis and Characterization of Gold Nanoparticles Functionalized with Butylated Hydroxytoluene Ligands

The in-house developing eight sulfur-containing BHT-ligands (S-BHTLs) were designed and synthesized as reported previously using acid catalyzed reaction by placing aryl and alkyl on para position of BHT without altering the phenolic ring of BHT structure as well as the dimerization of BHT on thiols [17]. The resulted enhanced radical scavenging and cancer-cytotoxic effects were encouraging. This current study is implemented to further explore the effects of novel hybridization with AuNPs on antioxidant and cancer toxicity and selectivity parameters.

The AuNPs was synthesized with the size ranging from 10 to 20 nm, which is suitable for drug delivery and offers less toxicity [23]. The S-BHTLs were functionalized with AuNPs to develop a novel nanoantioxidant stems from nanotechnology (AuNPs) and supramolecular chemistry (Sulfur-containing BHT ligands, S-BHTLs) in accomplishing the amplified antioxidant activity (Figure 1). Thiols as terminal of S-BHTLs are highly polarizable and strong electron-releasing ligands meanwhile Au is soft lewis acid. Thus, the interaction between thiols and Au formed a very stable metal colloid due to the strong bonding between these two elements. Furthermore, the Van der Waals interaction between thioether and AuNPs also played a significant role in the formation of nanocomposites [24].

Figure 2 shows the TEM image of the synthesized AuNPs and thiolated-AuNPs at high magnification. The size of AuNPs used in this study was about 11 to 12 nm as illustrated in Figure 2 (a) before functionalization. The data confirmed that the synthesized AuNPs were in the range of 10 – 20 nm as planned with BHTLs functionalized with AuNPs. The size still remains in the range 10 to 20 nm after the functionalization with Au-S-BHTLs as illustrated in Figure 2 (b). The result indicated that the attachment of S-BHTLs on the surface of AuNPs did not change the size of nanoparticles. Moreover, Figure 2 (c) and 2 (d) illustrate the high-resolution image of lattice fringes of AuNPs with crystallite size is 0.233 nm before functionalization and 0.231 nm after functionalization. This size is corresponding to lattice spacing between the (111) plane of face centered cubic (fcc) of AuNPs (0.235 nm) (JCPDS card No: 04-0784). Thus, this shows that the crystallite size does not change after functionalization with Au-S-BHTLs [25].

The morphology of AuNPs before and after functionalization with S-BHTLs was carried out by SEM (Figure 3) including the EDX spectra of all nanocomposites (Figure 4). The image of

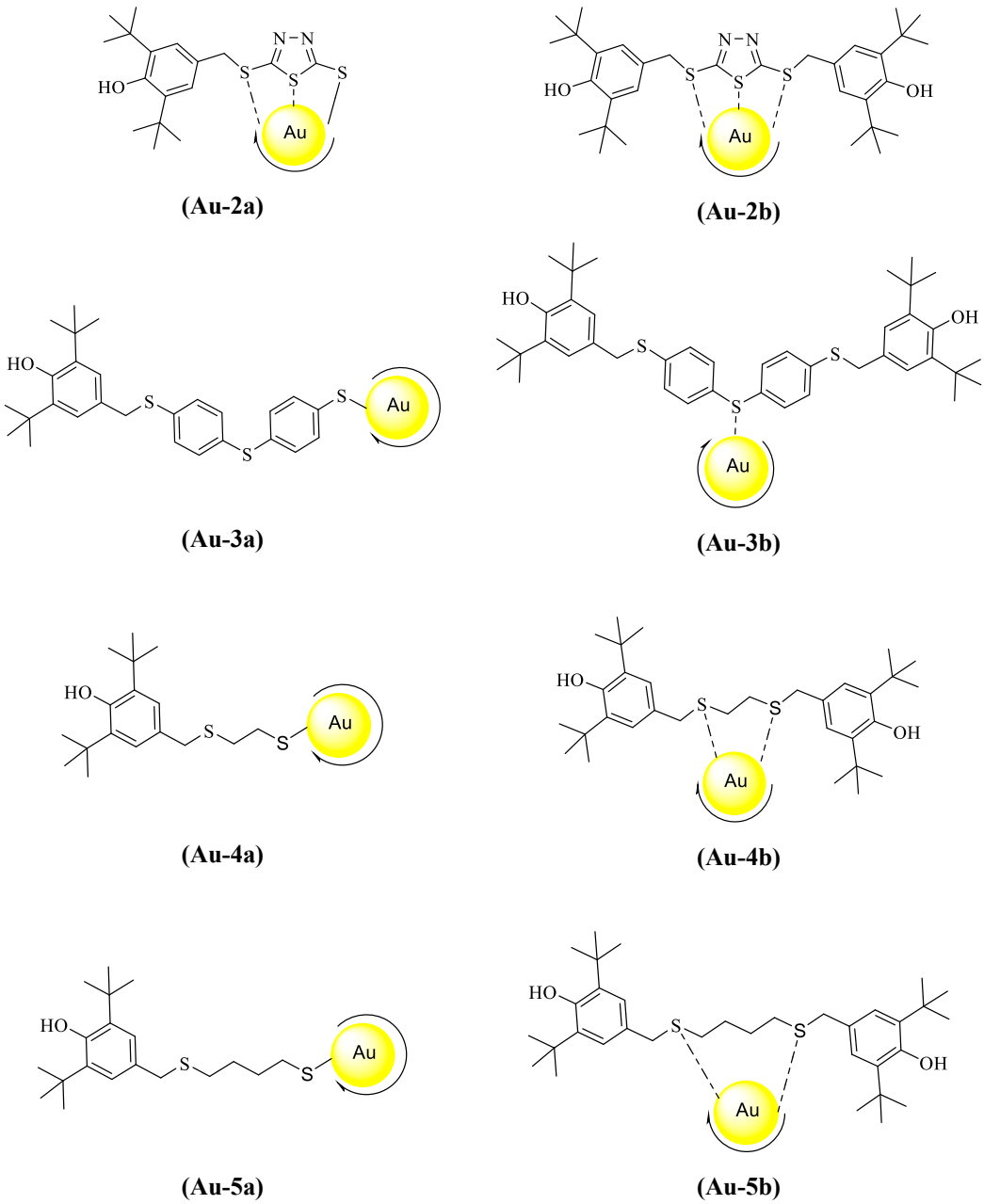

Figure 1. Molecular structures of nanocomposites.

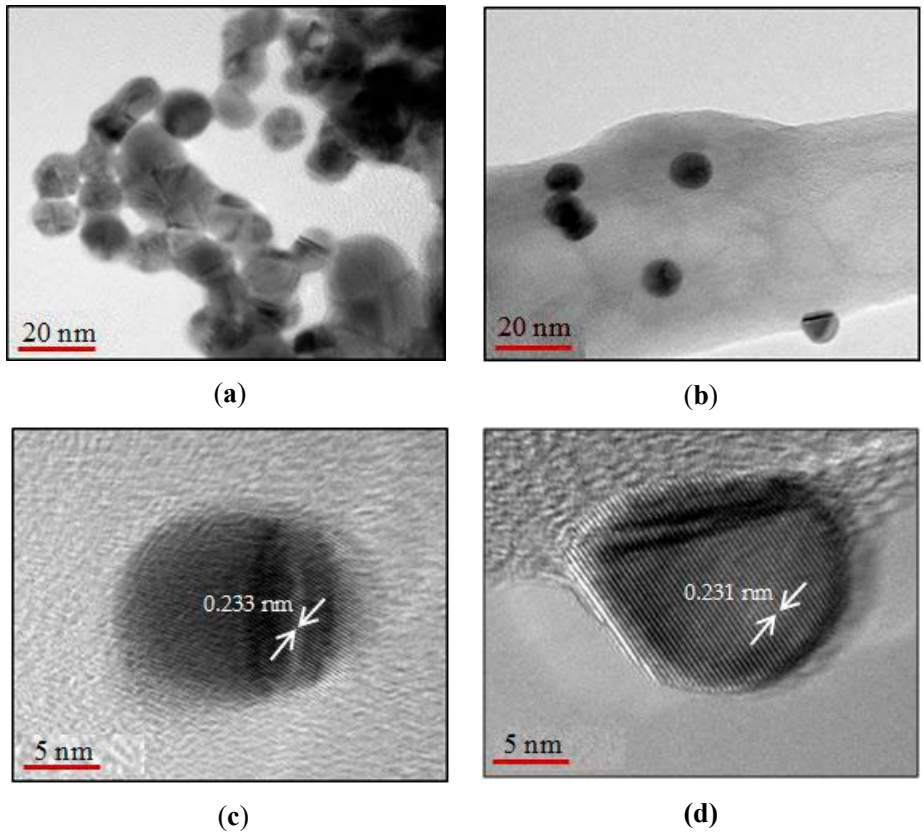

Figure 2. TEM images of gold nanoparticles before functionalization (**a**), after functionalization with Au-S-BHTLs (**b**), crystallite size before (**c**) and crystallite size after functionalization (**d**).

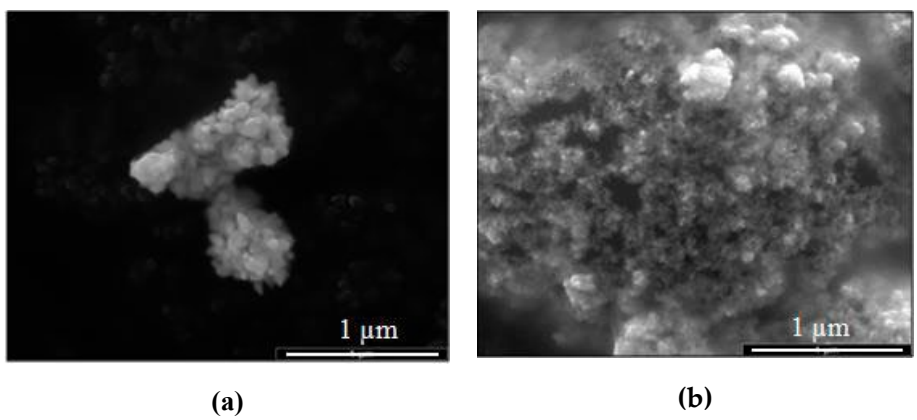

Figure 3. The FESEM images **AuNPs** before functionalization with S-BHTLs (**a**) and **AuNPs** after functionalization with S-BHTLs (**b**).

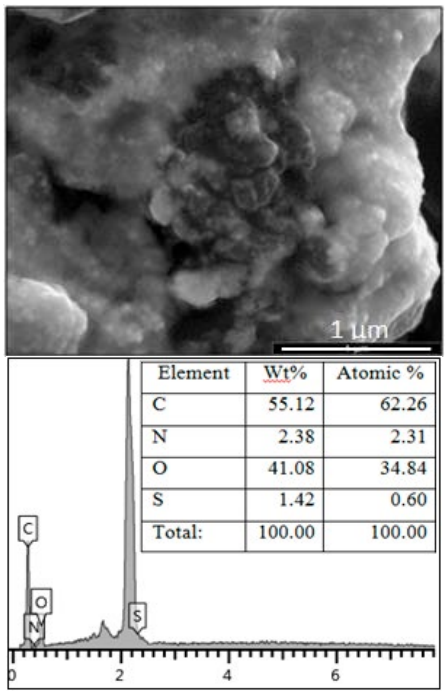

Element	Wt%	Atomic %
C	55.12	62.26
N	2.38	2.31
O	41.08	34.84
S	1.42	0.60
Total:	100.00	100.00

(a) **Au-2a**

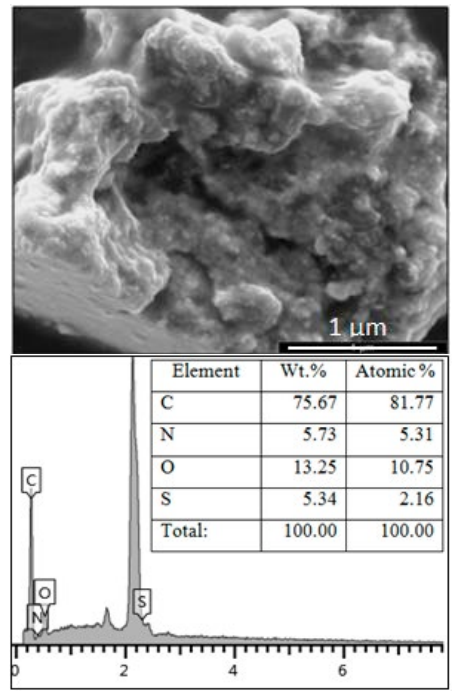

Element	Wt.%	Atomic %
C	75.67	81.77
N	5.73	5.31
O	13.25	10.75
S	5.34	2.16
Total:	100.00	100.00

(b) **Au-2b**

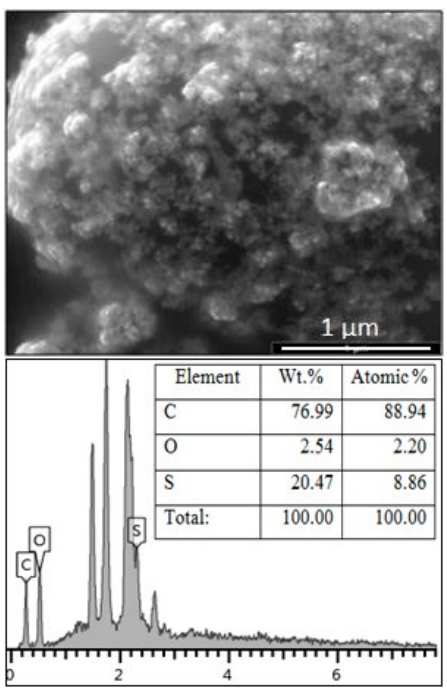

Element	Wt.%	Atomic %
C	76.99	88.94
O	2.54	2.20
S	20.47	8.86
Total:	100.00	100.00

(c) **Au-3a**

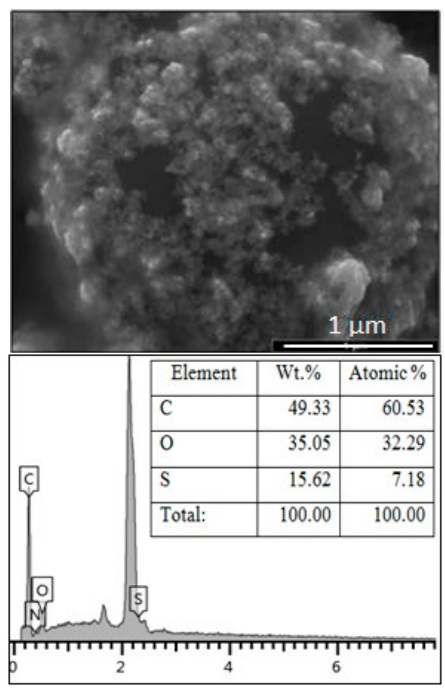

Element	Wt.%	Atomic %
C	49.33	60.53
O	35.05	32.29
S	15.62	7.18
Total:	100.00	100.00

(d) **Au-3b**

Figure 4. For legend, see the following page.

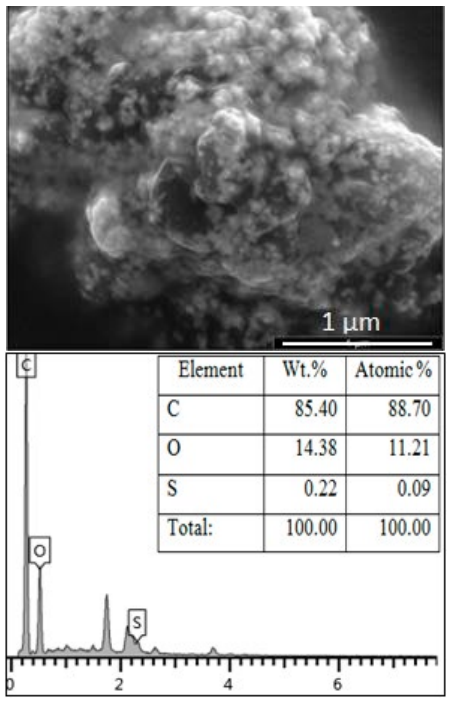

Element	Wt.%	Atomic %
C	85.40	88.70
O	14.38	11.21
S	0.22	0.09
Total:	100.00	100.00

(e) **Au-4a**

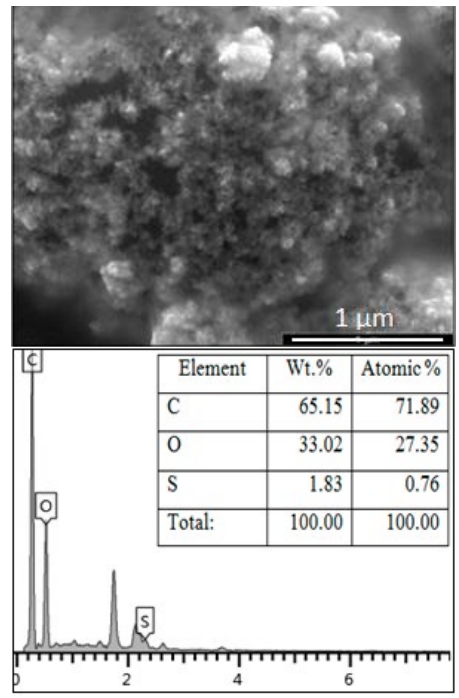

Element	Wt.%	Atomic %
C	65.15	71.89
O	33.02	27.35
S	1.83	0.76
Total:	100.00	100.00

(f) **Au-4b**

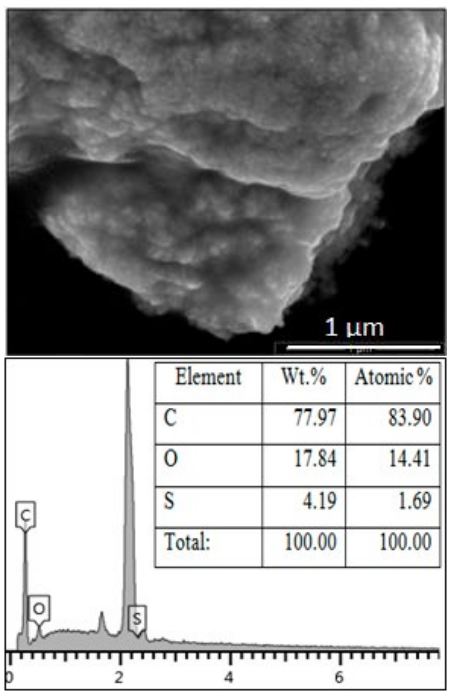

Element	Wt.%	Atomic %
C	77.97	83.90
O	17.84	14.41
S	4.19	1.69
Total:	100.00	100.00

(g) **Au-5a**

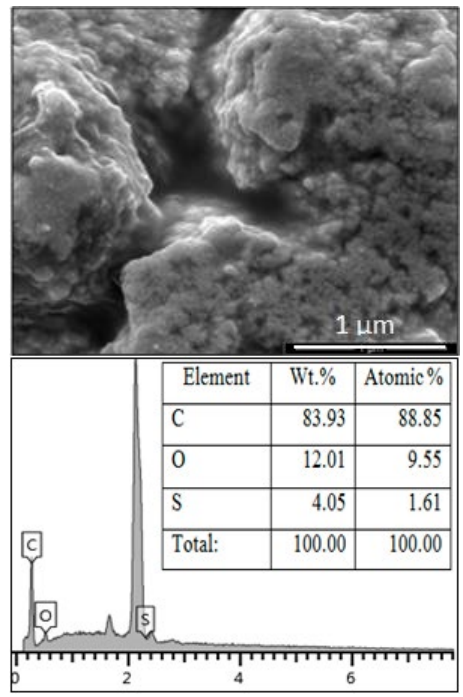

Element	Wt.%	Atomic %
C	83.93	88.85
O	12.01	9.55
S	4.05	1.61
Total:	100.00	100.00

(h) **Au-5b**

Figure 4. (Continued)The FESEM images including EDX spectra of **Au-2a** (a), **Au-2b** (b), **Au-3a** (c), **Au-3b** (d), **Au- 4a** (e), **Au-4b** (f), **Au-5a** (g) and **Au-5b** (h).

AuNPs before functionalization demonstrates the formation of nanoparticles in nanosphere shape and agglomerate by each other as in Figure 3(a). This is due to high surface charge density and all particles are attracting to each other to prevent any undesirable reaction [26]. On the other hand, thiolated-AuNPs remained spherical in shape and uniformly scattered after functionalization with antioxidant groups as described in Figure 3(b). This reveals that the functionalization of S-BHTLs on the AuNPs does not change the shape of nanoparticles. Also, it may indicate the possible dispersion stability after the phenolic functionalization on AuNPs surface, as cited previously [27].

The EDX analysis report the appearance of S-BHTLs on the surface of AuNPs for nanocomposites of compounds "**a**" and "**b**" as shown in Figure 4. It shows the appearance of all elements contained in S-BHTLs. The **Au-3a** and **Au-3b** exhibited the appearance of carbon (C), oxygen (O), and S elements. The **Au-2a** and **Au-2b** also reported the same elements as contained in **Au-3a** with additional element of nitrogen, N. The **Au-4a**, **Au-4b**, **Au-5a** and **Au-5b** reported the appearance of all element as the same as **Au-3a**. These eight data groups strongly supported the functionalization of S-BHTLs on the surface of AuNPs, similar to previous findings using organic ligands on AuNPs surface [28]. The data were also supported by the antioxidant activity results which demonstrate that the functionalization of S-BHTLs on the surface of AuNPs was successful.

UV spectra in Figure 5 show the absorption peak of AuNPs and Au-S-BHTLs. The AuNPs have the absorbance peak at wavelength of 520 nm due to the excitation of surface plasmon vibrations. After functionalization of S-BHTLs on AuNPs surface, the peak at wavelength range 510 to 530 nm disappeared and another absorbance peak appeared at 324 nm, which was related with conjugation of S-BHTLs on AuNPs surface. This absorbance peak shows that the presence of ligands on AuNPs surface, which is in accordance with data previously reported by Ngo et al [29].

FT-IR spectra (Figure 6) show clear evidence that S-BHTLs forms part of the nanocomposites. Figure 6a displays the terminal thiol, -SH appeared at peak 2533.1 cm^{-1}. Nonetheless, this peak disappeared after functionalization (Figure 6b). This is strong evidence that the ligands are successfully attached on the surface of nanoparticles [30]. The

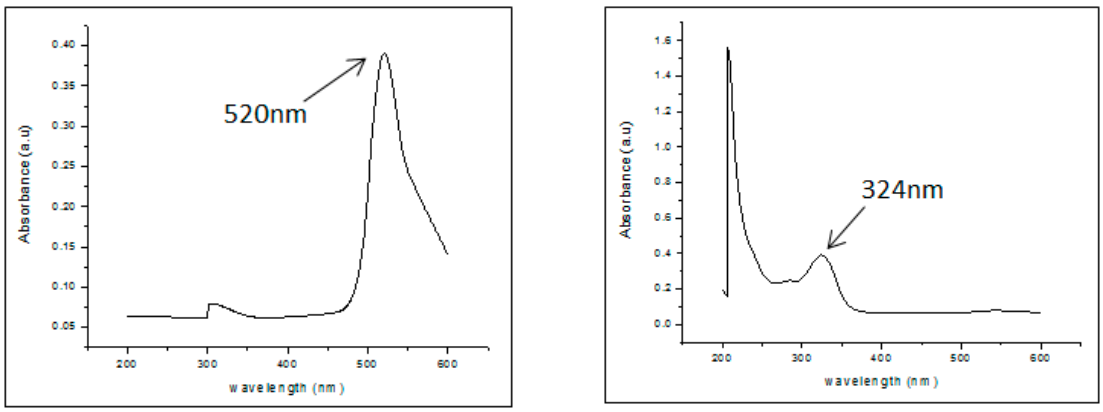

(**a**) (**b**)

Figure 5. UV-Vis spectra of AuNPs (**a**) and Au-S-BHTLs (**b**).

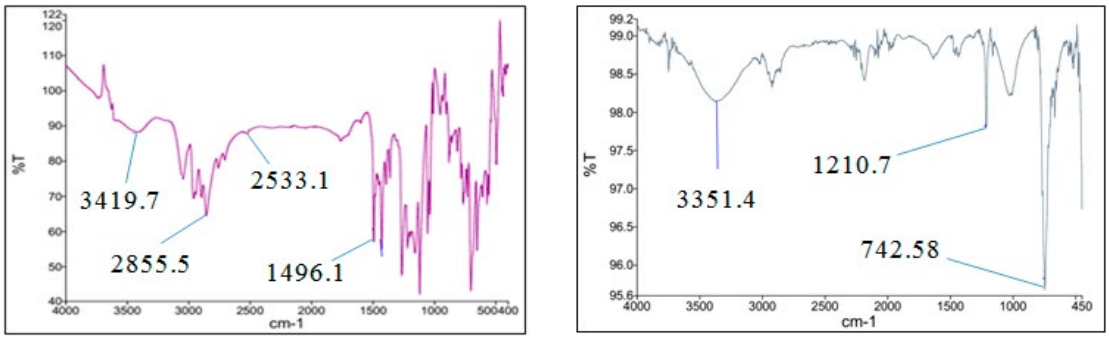

(**a**) (**b**)

Figure 6. FT-IR spectra of ligands (**a**) and Au-ligands (**b**).

formation of thiolate-Au bond between ligands and the Au surface was identified by the absence of an S-H stretching mode of Au-S-BHTLs in the IR spectrum [31].

3.2 Antioxidant Activity

The hydrogen donating capacity of the compound was reflected by the antioxidant effects in the DPPH-radical-scavenging assay. The DPPH$^{\bullet}$ radical absorbed at 517nm in its radical form. The DPPH radical form was scavenged to form a stable DPPH molecule by antioxidant entity through the protonation of a hydrogen atom. This leads to decreasing in absorbance by color change from purple to yellow [32, 33]. In our previous work [17], we have reported the enhanced antioxidant activities of many S-BHTLs structures compared to the free BHT control. In this current study, we have further developed the synthesized structures with nano-hybridization using AuNPs moieties and examined the effect on antioxidant activity.

Table 1 shows the radical scavenging activity of S-BHTLs and Au-S-BHTLs compared to BHT and un-functionalized AuNPs with the percentage change of IC_{50}, respectively. Results show that most of S-BHTLs showed the stronger antioxidant activity with lower IC_{50} compared to standard BHT. As reported previously by our team [17], the ligand **2b** showed more potent antiradical properties against DPPH radical with IC_{50} value of 11.0 ± 0.26 μg/ml, 47.9% lower compared to standard BHT, followed by ligand **5a** showed moderate activity with 9.5% increase IC_{50} value (23.1 ± 0.25 μg/ml) than standard BHT.

Then, after functionalization with AuNPs, the majority of Au-S-BHTLs exhibited lower IC_{50} values compared to the un-functionalized AuNPs. In this case, the thiolated-Au, **Au-5a** displayed the highest radical inhibition with IC_{50} value of 39.7 ± 0.87 μg/ml and 66% decrease, followed by **Au-3a** with 55.9 ± 0.68 μg/ml and 52.1% decrease compared to un-functionalized AuNPs. Results indicate that the nanocomposites containing long chain aliphatic thiol ligand such as ligand **5a** exhibited stronger scavenging effect against free radical entity, followed by diaryl sulfide which had long chain with a formation of two benzene rings joined together by sulfur bridge. The structure activity relationship showed that the long chain aliphatic thiol allowed lots of number of antioxidant group to attach on the surface and increased the antioxidant ability of nanomaterial [34]. Meanwhile, the aromatic thiol has limited number of ligands attachment due the higher electron cloud density from the ring compared to aliphatic thiol [35].

Table 1. The IC_{50} values of the synthesized S-BHTLs, [17] and Au-S-BHTLs compounds against DPPH radical.

Comp. no	Scavenging activity DPPH of S-BHTLs (IC_{50} μg/mL), [17]	% change of IC50 of S-BHTLs, compared to BHT, [17]	Scavenging activity DPPH of Au-S-BHTLs (IC_{50} μg/ml)	% change of IC50 of Au-S-BHTLs, compared to Au
2a	14.1 ± 0.30	-33.2%	161.9 ± 0.60	38.4%
2b	11.0 ± 0.26	-47.9%	94.1 ± 0.84	-19.5%
3a	14.3 ± 0.31	-32.2%	55.9 ± 0.68	-52.1%
3b	12.1 ± 0.15	-42.7%	97.1 ± 0.49	-16.9%
4a	23.2 ± 0.35	9.9%	110.7 ± 0.98	-5.3%
4b	15.4 ± 0.29	-27.0%	122.8 ± 0.88	5.0%
5a	23.1 ± 0.25	9.5%	39.7 ± 0.87	-66.0%
5b	17.2 ± 0.21	-18.4%	215.4 ± 0.70	84.2%
Au	-	-	116.9 ± 0.75	-
BHT	21.1 ± 0.40	-	-	-

[1] Each value represents the mean ± standard deviation of triplicates.

3.3 Cell Viability

The synthesized S-BHTLs and Au-S-BHTLs were evaluated for their cytotoxicity in two different cancer cell lines: colon adenocarcinoma (HT-29) and breast adenocarcinoma (MCF-7). They were also tested for their cytotoxicity properties in non-tumorigenic cells which are non-tumor colon cell (CCD 841) and breast cell (MCF10A) to indetify the selectivity index. The values of IC_{50} for S-BHTLs and Au-BHTLs are shown in Table 2 and Table 3, respectively which are calculated from the cell viability dose response curves obtained after 24-hour drug treatment in the MTT assay. As reported previously by our team [17], ligand **2b** displayed highest cytotoxic effect against HT29 and MCF7 cancer cell lines with IC_{50} value of 28.0 ± 1.67 μg/ml and 14.1 ± 1.02 μg/ml, respectively as shown in Table 2. It also showed superior selectivity index in colon (SI=5.14) and breast (SI=13.85) tissues. Meanwhile, aliphatic thiol ligand, **5a** showed moderate cytotoxicity activity against HT29 (200.9 ± 11.66 μg/ml) and MCF7 (220.3 ± 14.91 μg/ml) cancer cells with lower selectivity index (SI<2.0).

After functionalization, all nanocomposites, Au-S-BHTLs showed stronger cytotoxic activity against HT29 cells with IC_{50} values lower than that of un-functionalized **AuNPs**, 193.93 ± 19.98 μg/ml except for nanocomposite **Au-4a** with IC_{50} value of 211.37 ± 34.51 μg/ml as reported in Table 3. Interestingly, nanocomposite **Au-2b** displayed a great potential with the most potent cytotoxic activity against MCF7 cells with a IC_{50} value of 40.59 ± 1.27 μg/ml in comparison to **AuNPs** (83.79 ± 4.83 μg/ml). Other compounds exhibited moderate inhibitory effect against HT29 cells and showed weak activity against MCF7 cancer cell lines. In cytotoxicity activity, the potency of "**b**" nanocomposites revealed that ligands with two BHT moieties exhibited excellent synergistic effect and higher activity compared to their one-side "**a**" counterparts [17] oppositely with antioxidant activity. In addition, the SI of majority of Au-S-BHTLs showed remarkable improvement

Table 2. The IC_{50} values of the synthesized sulphur-containing BHT ligands, S-BHTLs compounds against HT29 and MCF7 cells after 24 hours incubation. [17]

Compound no	IC_{50} µg/mL					
	HT29	CCD 841	SI	MCF7	MCF10A	SI
2a	76.0 ± 6.20	128.4 ± 7.64	1.69	103.8 ± 2.35	238.7 ± 6.87	2.29
2b	28.0 ± 1.67	143.9 ± 2.07	5.14	14.1 ± 1.02	174.4 ± 5.32	13.85
3a	257.4 ± 12.90	>400	>1.55	342.6 ± 1.33	328.9 ± 1.37	0.96
3b	266.1 ± 14.22	313.9 ± 8.79	1.18	170.5 ± 5.95	231.9 ± 18.41	1.36
4a	320.8 ± 6.49	225.1 ± 8.41	0.70	278.8 ± 6.63	200.7 ± 8.67	0.72
4b	325.2 ± 5.23	289.4 ± 15.94	0.89	160.2 ± 5.34	257.9 ± 11.59	1.61
5a	200.9 ± 11.66	255.1 ± 6.42	1.27	220.3 ± 14.91	198.3 ± 9.16	0.90
5b	290.2 ± 14.58	296.0 ± 12.78	1.02	241.8 ± 14.57	212.8 ± 3.94	0.88
BHT	312.1 ± 10.03	252.8 ± 8.25	0.81	134.9 ± 11.02	192.9 ± 7.24	1.43

[1] Each value represents the mean ± standard deviation of triplicates; BHT = Butylated Hydroxytoluene; SI = Selectivity Index.

Table 3. The IC_{50} values of the synthesized nanocomposites, Au-S-BHTLs compounds against HT29 and MCF7 cells after 24 hours incubation.

Compound no	IC_{50} µg/ml					
	HT29	CCD 841	SI	MCF7	MCF10A	SI
Au-2a	57.35 ± 1.82	400.02 ± 32.06	6.98	89.15 ± 11.87	435.70 ± 10.63	4.89
Au-2b	50.08 ± 3.01	777.41 ± 15.98	15.52	40.59 ± 1.27	400.16 ± 35.83	9.86
Au-3a	181.22 ± 30.06	>1000	>5.52	139.67 ± 19.43	>1000	>7.15
Au-3b	187.08 ± 46.19	666.11 ± 26.92	3.56	118.98 ± 23.27	466.27 ± 14.81	3.92
Au-4a	211.37 ± 34.51	423.47 ± 12.53	2.01	284.03 ± 35.72	>1000	>3.52
Au-4b	99.50 ± 2.05	>1000	>10.05	167.58 ± 10.38	>1000	>5.97
Au-5a	166.62 ± 41.96	617.14 ± 16.28	3.70	249.77 ± 27.27	578.10 ± 24.04	2.31
Au-5b	185.54 ± 38.87	656.95 ± 19.17	3.54	290.05 ± 3.39	542.97 ± 35.10	1.87
Au	193.93 ± 19.98	555.67 ± 60.56	2.87	83.79 ± 4.83	>1000	>11.93

[1] Each value represents the mean ± standard deviation of triplicates; Au = Gold; SI = Selectivity Index.

surpassing the safety threshold ≥ 2.0 as reported previously [36], which in turn confirm the role of Au in securing selective anti-cancer activity.

Results indicate that the presence of thiadiazole in both S-BHTLs and Au-S-BHTLs demonstrated a high cytotoxic potency due to its aromaticity as good electron donor [37]. Previous works also suggested the influence of tertiary amine improving cytotoxicity in cancer cells are attributed to its electron donating ability [38]. The presence of electronegativity elements on the molecular structure gives strong effect on cytotoxicity activity of S-BHTLs and Au-S-BHTLs with excellent SI values. This is because the increased number of sulfur and nitrogen elements on the structure is increasing the aromaticity of heterocyclic ring [39]. Moreover, the combination of S-BHTLs with AuNPs was significantly enhanced the cytotoxicity effect and improved the selectivity index of conjugated ligands as promising selective anticancer agent in cancer therapy [40].

4. Conclusions

This study successfully developed novel nanoantioxidant stems from S-BHTLs functionalized with AuNPs (Au-S-BHTLs) by incorporating thiol ligands derived from BHT. This strategy improves the antioxidant abilities of nanomaterial as free radical scavenging compound. The monomerization of BHT with aliphatic thiols shows good antioxidant activity due to the formation of bulky long chain on the surface of nanoparticles. Meanwhile, the dimerization of BHT with sulfur-containing compounds is less promising as free radical scavenger due to lower packing density of antioxidant molecules. Our results show that the antioxidant activity of the assembly of BHT-thiol ligands on AuNPs are varied due to bulky antioxidants, which presents a novel perspective and understanding on nanoantioxidant as well as the chemistry behind the antioxidant activities of Au-S-BHTLs. Thus, this study proves that the packing density does not significantly affect the cytotoxicity of nanocomposites and reveals that the aromaticity of heterocyclic ring gives strong cytotoxic effect on cancer cell lines.

Acknowledgements

The authors wish to acknowledge the grant (FP050-2014B and FP127-2019A) provided by Ministry of Higher Education Malaysia and Post-graduate Research Grant (PPP-2015B) provided by University of Malaya to conduct this study.

Conflict of interest statement

The authors declare no conflict of interest. The funders had no role in the design of the study; in the collection, analyses, or interpretation of data; in the writing of the manuscript, or in the decision to publish the results.

References

[1] Dugger S.A., Platt A. and Goldstein D.B., *Nat. Rev. Drug Discov.,* 2018; **17**: 183-196. DOI 10.1038/nrd.2017.226.

[2] Brash D.E., Rudolph J.A., Simon J.A., Lin A., McKenna G.J., Baden H.P., Halperin A.J. and Pontén J., *Proc. Natl. Acad. Sci. USA.,* 1991; **88**: 10124-10128. DOI 10.1073/pnas.88.22.10124.

[3] Ariffin A., Rahman N.A., Yehye W.A., Alhadi A.A. and Kadir F.A., *Eur. J. Med. Chem.,* 2014; **87**: 564-577. DOI 10.1016/j.ejmech.2014.10.001.

[4] Elmadfa I. and Meyer A.L., *Ann. Nutr. Metab.,* 2008; **52**: 2-5. DOI 10.1159/000115339.

[5] Kadir F.A., Kassim N.M., Abdulla M.A. and Yehye W.A., *BMC Complement. Altern. Med.,* 2013; **13**: 343. DOI 10.1186/1472-6882-13-343.

[6] Sandhiya S., Dkhar S.A. and Surendiran A., *Fundam. Clin. Pharmacol.,* 2009; **23**: 263-269. DOI 10.1111/j.1472-8206.2009.00692.x.

[7] Hu Q., Li H., Wang L., Gu H. and Fan C., *Chem. Rev.,* 2018; **119**: 6459-6506. DOI 10.1021/acs.chemrev.7b00663.

[8] Tran S., DeGiovanni P.-J., Piel B. and Rai P., *Clin. Transl. Med.,* 2017; **6**: 44. DOI 10.1186/s40169-017-0175-0.

[9] Garza M.D.L., Lopez I. and Gomez I., *Adv. Mater. Sci. Eng.,* 2013; **2013**: 916908. DOI 10.1155/2013/916908.

[10] Jain S., Hirst D. and O'Sullivan J., *Br. J. Radiol.,* 2012; **85**: 101-113. DOI 10.1259/bjr/59448833.

[11] Fernandez-Moreira V., Herrera R.P. and Gimeno M.C., *Pure Appl. Chem.,* 2019; **91**: 247-269. DOI 10.1515/pac-2018-0901.

[12] Kouodom M.N., Boscutti G., Celegato M., Crisma M., Sitran S., Aldinucci D., Formaggio F., Ronconi L. and Fregona D., *J. Inorg. Biochem.,* 2012; **117**: 248-260. DOI 10.1016/j.jinorgbio.2012.07.001.

[13] Liu B. and Liu J.W., *Anal. Methods,* 2017; **9**: 2633-2643. DOI 10.1039/c7ay00368d.

[14] Manea F., Houillon F.B., Pasquato L. and Scrimin P., *Angew. Chem. Int. Edit.,* 2004; **43**: 6165-6169. DOI 10.1002/anie.200460649.

[15] Selim M.E. and Hendi A.A., *Asian Pac. J. Cancer P.,* 2012; **13**: 1617-1620. DOI 10.7314/APJCP.2012.13.4.1617.

[16] Safwat M.A., Soliman G.M., Sayed D. and Attia M.A., *Int. J. Pharm.,* 2016; **513**: 648-658. DOI 10.1016/j.ijpharm.2016.09.076.

[17] Ahmad M.H., Rahman N.A., Kadir F.A., Al-Ani L.A., Hashim N.M. and Yehye W.A., *J. Chem. Sci.,* 2019; **131**: 107. DOI 10.1007/s12039-019-1682-x.

[18] Li N., Yu L. and Zou J., *J. Lab. Autom.,* 2014; **19**: 82-90. DOI 10.1177/2211068213498240.

[19] Gao J., Huang X., Liu H., Zan F. and Ren J., *Langmuir,* 2012; **28**: 4464-4471. DOI 10.1021/la204289k.

[20] Gorinstein S., Martin-Belloso O., Katrich E., Lojek A., Ciz M., Gligelmo-Miguel N., Haruenkit R., Park Y.S., Jung S.T. and Trakhtenberg S., *J. Nutr. Biochem.,* 2003; **14**: 154-159. DOI 10.1016/S0955-2863(02)00278-4.

[21] Tsuzuki Y., Carreira C.M., Bockhorn M., Xu L., Jain R.K. and Fukumura D., *Lab. Invest.,* 2001; **81**: 1439-1451. DOI 10.1038/labinvest.3780357.

[22] Badisa R.B., Ayuk-Takem L.T., Ikediobi C.O. and Walker E.H., *Pharm. Biol.,* 2006; **44**: 141-145. DOI 10.1080/13880200600592301.

[23] Adewale O.B., Davids H., Cairncross L. and Roux S., *Int. J. Toxicol.,* 2019; **38**: 357-384. DOI 10.1177/1091581819863130.

[24] Reimers J.R., Ford M.J., Marcuccio S.M., Ulstrup J. and Hush N.S., *Nat. Rev. Chem.,* 2017; **1**: 0017. DOI 10.1038/s41570-017-0017.

[25] Majeed J., Ramkumar J., Chandramouleeswaran S. and Tyagi A.K., *Sep. Sci. Technol.,* 2020; **55**: 1922-1931. DOI 10.1080/01496395.2019.1617746.

[26] Ashraf M.A., Peng W., Zare Y. and Rhee K.Y., *Nanoscale Res. Lett.,* 2018; **13**: 214. DOI 10.1186/s11671-018-2624-0.

[27] Irfan M., Ahmad T., Moniruzzaman M., Bhattacharjee S. and Abdullah B., *Arab. J. Chem.,* 2020; **13**: 75-85. DOI 10.1016/j.arabjc.2017.02.001.

[28] Banihashem S., Nezhati M.N. and Panahia H.A., *Carbohydr. Polym.,* 2020; **227**: 115333. DOI 10.1016/j.carbpol.2019.115333.

[29] Ngo V.K.T., Nguyen H.P.U., Huynh T.P., Tran N.N.P., Lam Q.V. and Huynh T.D., *Adv. Nat. Sci. Nanosci. Nanotechnol.,* 2015; **6**: 035015. DOI 10.1088/2043-6262/6/3/035015.

[30] Shahrivari S., Faridbod F. and Ganjali M.R., *Spectrochim. Acta A.,* 2018; **191**: 189-194. DOI 10.1016/j.saa.2017.09.064.

[31] Templeton A.C., Wuelfing W.P. and Murray R.W., *Accounts Chem. Res.,* 2000; **33**: 27-36. DOI 10.1021/ar9602664.

[32] Chen F., Huang G., Yang Z. and Hou Y., *Int. J. Biol. Macromol.,* 2019; **138**: 673-680. DOI 10.1016/j.ijbiomac.2019.07.129.

[33] Akar Z., Küçük M. and Doğan H., *J. Enzym. Inhib. Med. Ch.,* 2017; **32**: 640-647. DOI 10.1080/14756366.2017.1284068.

[34] Rambukwella M., Sakthivel N.A., Delcamp J.H., Sementa L., Fortunelli A. and Dass A., *Front. Chem.,* 2018; **6**: 330. DOI 10.3389/fchem.2018.00330.

[35] Nimmala P.R. and Dass A., *J. Am. Chem. Soc.,* 2014; **136**: 17016-17023. DOI 10.1021/ja5103025.

[36] Badisa R.B., Darling-Reed S.F., Joseph P., Cooperwood J.S., Latinwo L.M. and Goodman C.B., *Anticancer Res.,* 2009; **29**: 2993-2996. DOI 0250-7005/2009$2.00+.40.

[37] Jakovljević K., Joksović M.D., Matić I.Z., Petrović N., Stanojković T., Sladić D., Vujčić M., Janović B., Joksović L., Trifunović S. and Marković V., *Med. Chem. Commun.,* 2018; **9**: 1679-1697. DOI 10.1039/C8MD00316E.

[38] Siim B.G., Hicks K.O., Pullen S.M., van Zijl P.L., Denny W.A. and Wilson W.R., *Biochem. Pharmacol.,* 2000; **60**: 969-978. DOI 10.1016/S0006-2952(00)00420-2.

[39] Yun B.X. and Kerim A., *J. Theor. Comput. Chem.,* 2018; **17**: 1850006. DOI 10.1142/S0219633618500062.

[40] Mioc M., Pavel I.Z., Ghiulai R., Coricovac D.E., Farcaş C., Mihali C.-V., Oprean C., Serafim V., Popovici R.A., Dehelean C.A., Shtilman M.I., Tsatsakis A.M. and Şoica C., *Front. Pharmacol.,* 2018; **9**: 429. DOI 10.3389/fphar.2018.00429.